Visual Neuroscience (2001), **18**, 541–547. Printed in the USA.

DOI: 10.1017.S095252380118404X

Encoding of both vertical and horizontal disparity in random-dot stereograms by Wulst neurons of awake barn owls

ANDREAS NIEDER AND HERMANN WAGNER

Lehrstuhl für Zoologie/Tierphysiologie, Institut für Biologie II, RWTH Aachen, Kopernikusstrasse 16, D-52074 Aachen, Germany

(RECEIVED September 11, 2000; ACCEPTED April 10, 2001)

Abstract

In binocular vision, the lateral displacement of the eyes gives rise to both horizontal and vertical disparities between the images projected onto the left and right retinae. While it is well known that horizontal disparity is exploited by the binocular visual system of birds and mammals to enable depth perception, the role of vertical disparity is still largely unclear. In this study, neuronal activity in the visual forebrain (visual Wulst) of behaving barn owls to vertical disparity was investigated. Single-unit responses to global random-dot stereograms (RDS) were recorded with chronically implanted electrodes and transmitted *via* radiotelemetry. Nearly half of the cells investigated (44%, 16/36) varied the discharge as a function of vertical disparity. Like horizontal-disparity tuning profiles, vertical-disparity tuning curves typically exhibited periodic modulation with side peaks flanking a prominent main peak, and thus, could be fitted well with a Gabor function. This indicates that tuning to vertical disparity was not caused by disrupting horizontal-disparity tuning *via* vertical stimulus offset, but by classical disparity detectors whose orientation tuning was tilted. When tested with horizontal in addition to vertical disparity, almost all cells investigated (92%, 12/13) were tuned to both kinds of disparity. The emergence of disparity detectors sensitive in two dimensions (horizontal and vertical) is discussed within the framework of the disparity energy model.

Keywords: Behaving owl, Visual forebrain, Stereopsis, Binocular energy neuron, Radiotelemetry

Introduction

Because of the lateral displacement of the eyes, image disparities are in principle horizontal (or parallel to the interocular axis, respectively). However, vertical binocular disparities between the left eye image and the right eye image also arise from this lateral displacement. If an observer is fixating a point F on a fronto-parallel surface (Fig. 1), vertical disparities are only absent for points which lie in either the median plane of the head or the plane of regard, both of them passing through the fixation point. Beyond those planes, however, vertical disparities (and horizontal disparities, of course) arise because images (e.g. point P in Fig. 1) are nearer to one eye than to the other. As a consequence, the angles of elevation (α and β in Fig. 1) measured in the two eyes are slightly different, that is, images are projected with vertical displacement onto the retinae of both eyes. Thus, the absolute vertical disparity of any point in space is defined as $\alpha - \beta$, the difference in the vertical elevations of that point on the retinae of the two eyes (Howard & Rogers, 1995). Depending on whether a point lies to the right or to the left of the meridian plane, the sign of vertical disparity changes. The vertical horopter is the spatial range of corresponding points for vertical disparities. Based on psychophysical findings in humans (e.g. Nakayama, 1977) and a neurophysiological study in cats and an owl (Cooper & Pettigrew, 1979), the vertical horopter is proposed to be a tilted line passing through the observer's fixation point and his feet. This might be an ecological adaptation, as it would allow the stereoscopic mechanisms to operate in the behaviorally relevant region of the lower visual field between the animal and its horizon (Cooper & Pettigrew, 1979).

Vertical disparity alone conveys no stereoscopic depth information and its role in stereopsis is still a matter of debate. While a computational approach by Mayhew and Longuet-Higgins (1982) proposed that vertical disparities may specify the absolute viewing distance, empirical data could not verify this hypothesis (Cumming et al., 1991). However, more recent psychophysical studies in humans (Rogers & Bradshaw, 1993; Bradshaw et al., 1996) demonstrated that vertical disparities can indeed be exploited to scale the perceived depth and size of stereoscopic surfaces, but only if the field of view was sufficiently large (70 × 70 deg fields). In addition to distance estimation, vertical disparities may also be used to control vertical vergence movements (Howard & Rogers, 1995).

The elaborate binocular system of the owl, which has evolved independently from the mammalian binocular pathways (Karten et al., 1973; Pettigrew, 1986), enables these birds to extract depth in global random-dot stereograms (van der Willigen et al., 1998). As a putative neural substrate for this capability, the vast majority of neurons in the visual Wulst signal horizontal disparity (Nieder & Wagner, 2000, 2001). The current study presents evidence that

Address correspondence and reprint requests to: Andreas Nieder, Center for Learning and Memory, Department of Brain and Cognitive Sciences, E25-236, Massachusetts Institute of Technology, 77 Massachusetts Avenue, Cambridge, MA 02139, USA. E-mail: nieder@mit.edu

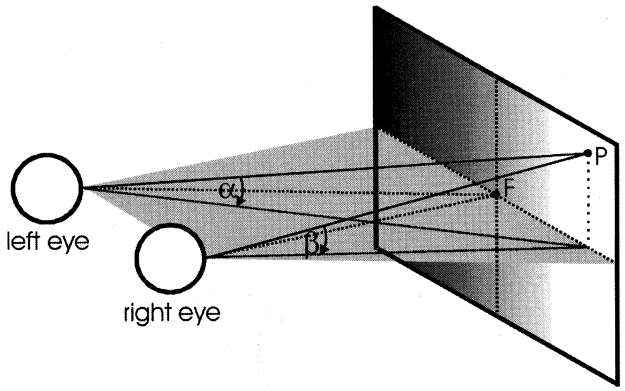

Fig. 1. Emergence of vertical disparity in binocular vision. An observer is fixating point F on a fronto-parallel surface. Point P on this surface is nearer to the right than to the left eye, and thus, the angles of elevation (α and β) in the two eyes are different. In fact, α is smaller than β, which equals a vertical displacement of point P relative to corresponding retinal images in the two eyes.

neurons in the visual Wulst of owls are also sensitive to vertical disparities in random-dot stereograms and encode disparity along both the vertical and horizontal dimension.

Methods

Behavioral task

A detailed description of the methods is given in Nieder and Wagner (2000). Briefly, two tame barn owls (*Tyto alba*) were trained on a visual fixation task. A bird was perched 57 cm in front of a CRT-screen and a fixation target (two lines, 0.8 deg long, 0.1 deg wide, and separated by 0.2 deg) was displayed whenever the owl oriented its gaze towards the screen. After a variable time delay (2–5 s), the fixation target turned 90 deg for 400 ms at which time the bird had to peck a key to get a reward. A small piece of meat supplied from a feeder served as reward. Eye and gaze orientation was qualitatively monitored on a TV monitor under infrared illumination at high magnification. In addition, an infrared reflex photoelectric device in combination with a light-reflexive foil attached at the top of the bird's head provided a two-dimensional threshold window to detect proper gaze orientation towards the screen, upon which the fixation target appeared. Tilted head positions did not trigger fixation target onset. A trial was interrupted whenever the bird made head movements larger than 1.5 deg. During the training, owls learned to avoid head movements while fixating and maintained a motionless, upright posture with the head straight up. Similar motionless fixation behavior has been observed previously in adult owls (Wagner & Schaeffel, 1991) and has been confirmed in experiments where owls were supplied with a head tracking device (van der Willigen, in preparation). Eye movements were not measured, as they are virtually absent in owls (Steinbach & Money, 1973; Pettigrew & Konishi, 1976*a*; du Lac & Knudsen, 1990). In a previous study (Nieder & Wagner, 2000), horizontal-disparity tuning curves were analyzed *post hoc* to confirm that data were not contaminated by vergence.

Surgical and recording procedures

For surgery, owls were given Valium (1 mg/kg) for sedation and ketamine (15 mg/kg/h) as an anesthetic. The skull was opened to expose the visuotopically organized forebrain representing the visual field adjacent to the area centralis (Pettigrew, 1979). Several custom-built microdrives supplied with one or two microelectrodes were fixed to the skull with dental cement. Tungsten microelectrodes (10 MΩ, FHC) were used to record single units. A metal bolt was fixed to the skull just above the beak to allow attachment of spectacles with filter glasses needed for stereoscopic stimulation. Wounds were closed and treated with antibiotic ointment. About 80% of the units were recorded extracellularly in the hyperstriatum accessorium (HA) of the visual Wulst, the remaining signals were recorded from intercalated nucleus (HIS) of the visual Wulst. Neuronal signals were transmitted with a custom-built stereo-radio transmitter (Nieder, 2000). Filtered (band-pass 500 Hz–5000 Hz, cutoff 12 dB/octave) and amplified signals were digitized at a sampling rate of 32 kHz and stored on a PC equipped with a Datawave Discovery package. Single units were isolated offline *via* cluster cutting. Recordings in awake animals avoided the risk of anesthesia artifacts (for visual neurons, see Lamme et al., 1998). Ketamine, the standard anesthetic in owls, is known to selectively antagonize NMDA receptors in the owl brain (Feldman et al., 1996). Moreover, to estimate zero disparity in a stereo task, the animal has to be awake and fixating (see discussion in Orban, 1991). Care and treatment of the owls were in accordance with the guidelines for animal experimentation as approved by the Regierungspäsidium Köln, Germany.

Visual stimulation

Visual stimulation was performed by means of a Silicon Graphics workstation. The color monitor (ELSA 17H96, 16″) had a spatial resolution of 1280 × 1024 pixels and was refreshed at a frame rate of 76 Hz in mono mode (used for receptive-field measurements). For stereoscopic presentations, the monitor was switched to stereo mode with a spatial resolution of 1280 x 496 pixels and a refresh rate of 120 Hz (60 frames/s for each eye). Stereoscopic presentation was accomplished using a liquid crystal polarizer (NuVision SGS17S) that was placed in front of the display. The polarizer allowed alternate transmission of images to the left and right eye with circularly opposite light polarization in synchrony with the monitor's refresh rate. In addition, the owls wore glasses that filtered polarized light to allow the passage of the right eye's image to the right eye while blocking it for the left eye and *vice versa*. Interocular crosstalk was about 11% (white stimulus).

A neuron's receptive field (RF) was mapped with moving bars. To construct disparity-response profiles, static random-dot stereograms (Julesz, 1960) covering the entire screen of the monitor around the fixation target were flashed for 500 ms. The random-dot stereograms (RDS) consisted of 10% white and 90% black dots. The size of the square dots was 0.15 deg. By shifting the dot patterns for the left and right eye vertically or horizontally, respectively, disparities were induced. Positive vertical disparity was defined as right-eye image above left-eye image. A new dot pattern was generated after each stimulus presentation. A sequence of 23 different disparity values centered symmetrically around zero disparity (±2.9 deg) was presented five to 15 times.

Data analysis

Average discharge rate was measured in a 500-ms time window (according to the stimulus' duration) that was shifted by 60 ms relative to stimulus onset. Disparity selectivity was statistically determined by calculating a nonparametric ANOVA (Kruskal

Wallis H-test; criterion: $P < 0.05$, two-tailed). To derive quantitative measures, a Gabor function (Gabor, 1946) was fitted (χ^2-minimization algorithms after Levenberg-Marquardt) to the response profiles derived from the mean firing rates as a function of disparity ($f(d)$).

$$f(d) = A * e^{-0.5\left(\frac{d-xc}{\sigma}\right)^2} * \cos\{2\pi[\omega(d - xc) + \phi]\} + B, \quad (1)$$

where A and B are the amplitude of the envelope and the firing rate offset (baseline), xc and σ are the position offset and the standard deviation of the Gaussian, and ω and ϕ are the frequency and phase of the cosine. Mean spike rate data points were weighted with standard errors when computing χ^2.

The disparity tuning index (DTI) of a tuning curve was determined by

$$DTI = \frac{(R_{max} - R_{min})}{(R_{min} + R_{max})}, \quad (2)$$

where R_{max} and R_{min} are the maximum and minimum mean spike rate, respectively.

Results

Vertical-disparity tuning profiles

The responses of 36 single units from two owls were tested for their sensitivity to vertical disparities in static random-dot stereograms (RDS). According to the statistical criterion described above, 44% (16/36) of the cells were significantly tuned to vertical disparities. Most vertical disparity-sensitive cells (11/16) showed a main excitatory response peak in the tuning curve; of those, seven units were tuned in the range of ±0.15 deg around zero disparity. The remaining vertical-disparity sensitive neurons (5/16) displayed strong inhibition at zero degree of vertical disparity. Four typical vertical-disparity response profiles are shown in Fig. 2. In Figs. 2A–2C, the tuning curves displayed a prominent peak near zero degree while the discharge was modulated on both sides of the peak until baseline activity was approached at very large and small vertical disparities, respectively. The cell in Fig. 2D, in contrast, showed maximum inhibition close to zero degree of vertical disparity and two excitatory peaks almost symmetrical around the zero-degree axis at approximately ±1 deg of vertical disparity.

Quantitative analysis of vertical-disparity tuning

Like horizontal-disparity tuning curves in owls (Nieder & Wagner, 2000), tuning profiles derived from vertical-disparity stimulation showed pronounced periodic modulation and a continuum of different shapes rather than discrete categories (see Fig. 2). Thus, no attempt was made to categorize tuning profiles according to the scheme suggested by Poggio and co-workers for horizontal-disparity tuning curves (see review by Poggio, 1995) that was also applied by Gonzalez et al. (1993) for vertical-disparity tuning curves of monkey visual-cortex cells. Instead, Gabor functions (the product of a Gaussian and a cosine) were fitted to vertical-disparity tuning profiles, as current models about disparity detection suggest Gabor-like tuning profiles (e.g. Ohzawa, 1998), and Gabor fits provided reasonable fits to horizontal-disparity tuning curves in the owl (Nieder & Wagner, 2000, 2001). On average, the

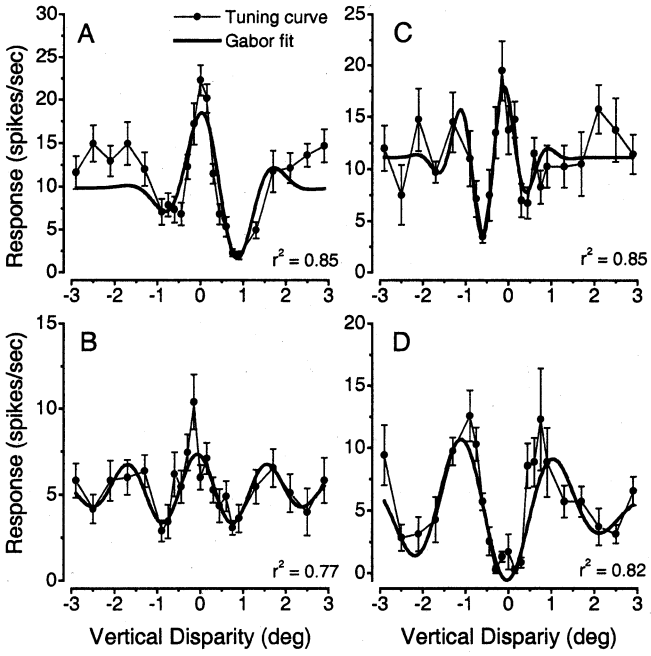

Fig. 2. Response profiles of four single units evoked by different vertical disparities in random-dot stereograms. Positive vertical disparity was defined as right-eye image above left-eye image. Lines with symbols represent neuronal responses (Error bars: ±SE), and thick lines indicate the Gabor fit (r^2 is the goodness of fit). (A–C) Neurons with a dominant tuning peak at zero degree of vertical disparity. (D) Single unit with almost complete suppression around zero degree but excitatory responses on both sides of the trough.

Gabor fits explained 71% of the neuronal vertical-tuning pattern (mean goodness of fit $r^2 = 0.71 \pm 0.13$), which is almost identical to the mean goodness of fit of 0.72 for horizontal disparity-tuning curves (Nieder & Wagner, 2000). The median for the most interesting parameters derived from the fits are as follows: Position of Gaussian (xc): −0.08 deg; sigma of Gaussian (σ): 0.67 deg; frequency of cosine (ϕ): 0.53 cycles/deg. As shown in Fig. 3, measures from vertical-disparity tuning curves were similarly distributed compared to parameters derived from horizontal-disparity profiles. No significant differences between the mean values could be detected when comparing xc, σ, and ϕ of vertical-disparity tuning curves with horizontal-disparity tuning curves (all $P \geq 0.2$, Mann–Whitney U test, two-tailed). Horizontal-disparity tuning data were taken from a previous study by Nieder and Wagner (2000). The phases of the fits, however, were more uniformly distributed for vertical-disparity tuning curves than for horizontal-disparity tuning profiles (Fig. 3D). Distribution of phases for vertical-disparity tuning curves showed no significant deviation from a uniform distribution ($P = 0.58$, one-sample Kolmogorov–Smirnov test), whereas phases of horizontal-disparity tuning profiles were significantly different from a uniform distribution ($P = 0.007$; data taken from Nieder & Wagner (2000)). It should be mentioned, however, that the sample size for vertical-tuning data ($n = 16$) was considerably smaller compared to the horizontal-tuning data ($n = 119$).

Tuning to both vertical and horizontal disparity

While horizontal disparity alone is sufficient for stereopsis and the vast majority of Wulst neurons encode horizontal displacements in

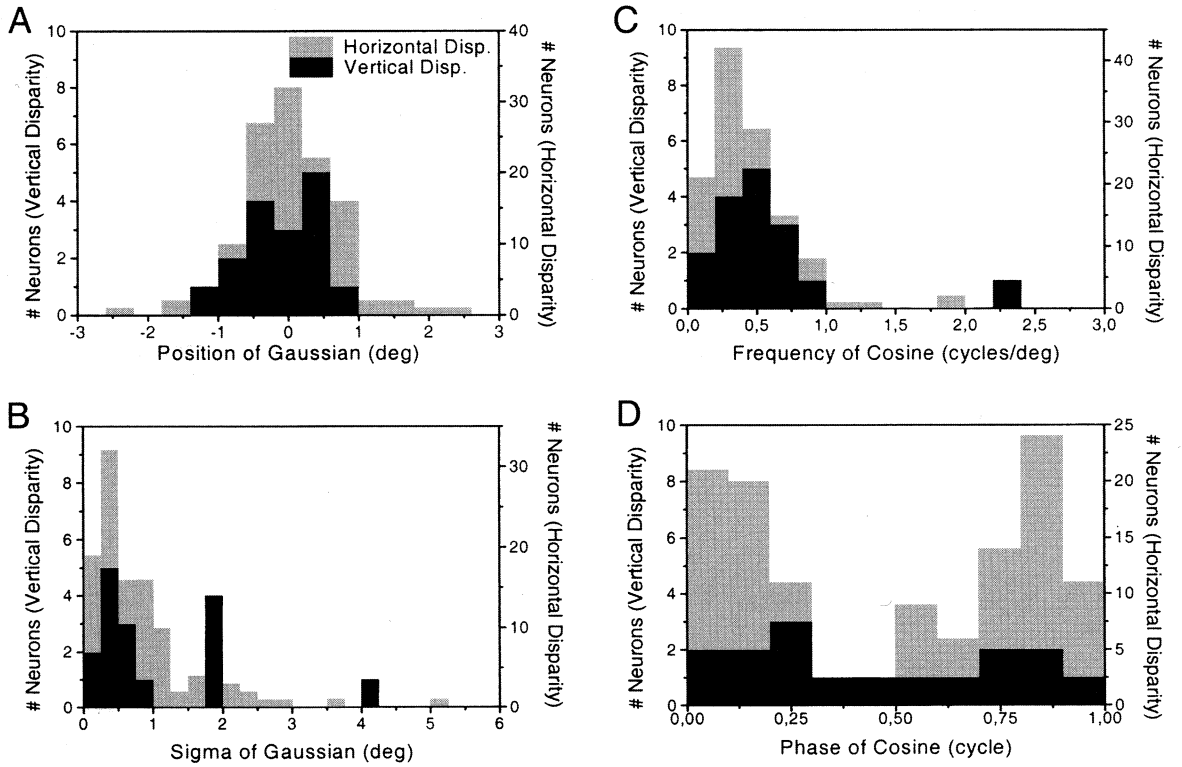

Fig. 3. Distribution of quantitative measures derived from Gabor fits. The peak of the Gaussian envelope (A), the disparity frequency (B), and the width of the Gaussian envelope (C) were comparable for vertical-disparity (black columns) and horizontal-disparity (gray columns) tuning curves. Only the phase of the profiles (D) were uniformly distributed for vertical-disparity tuning curves. Note the difference in the sample size for vertical- and horizontal-disparity tuning curves. Data for horizontal-disparity tuning were taken from Nieder and Wagner (2000).

RDS, vertical disparity can greatly influence depth perception. To test interactions, 13 of the 16 vertical-disparity sensitive cells were additionally examined for tuning to horizontal disparity in RDS. All but one cell (12/13) were tuned to both vertical and horizontal disparity. A neuron tested with both vertical and horizontal disparity is shown in Fig. 4. This unit was excitatory tuned to a restricted range for both horizontal and vertical disparities. Note that although the profiles look almost identical, the maximum discharge occurred at different vertical- and horizontal-disparity values, as horizontal disparity was set to the preferred disparity of -0.75 deg when measuring vertical disparity. The plot illustrates that such neurons have a two-dimensional response map with vertical and horizontal disparity as dimensions.

The preferred disparities of the 12 neurons tuned to vertical and horizontal disparity are plotted in Fig. 5A. (Preferred disparity was determined as maximum discharge to any disparity value, except for three "tuned inhibitory" units where the preferred disparity was determined as response minimum.) The distribution of preferred vertical disparities seemed to be more narrow compared to the distribution of preferred horizontal disparities. The disparity tuning index (a measure of the response strength, see Methods) of the cells (Fig. 5B) tended to be correlated for vertical and horizontal disparity (Pearson correlation, $r = 0.56$, $P = 0.06$).

According to the restriction of the cells' monocular receptive fields (RF), a neuron tuned for horizontal disparity (by means of vertical orientation preference of its monocular subunits) must necessarily be tuned for vertical disparity (and *vice versa*). If two dots move far enough apart on the vertical axis in one eye relative to the other, discharge of any binocular cell will be altered, thus causing "tuning" in the vertical-disparity response profile. "True" vertical-disparity tuning, however, arises for neurons whose monocular subunits prefer horizontal stimulus orientation. In this case,

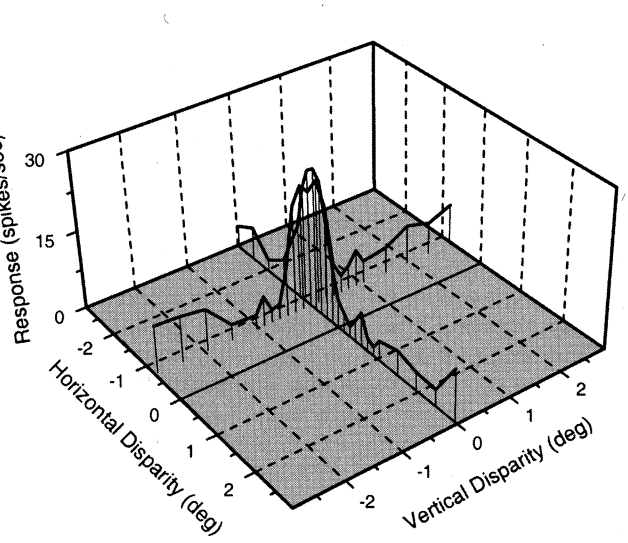

Fig. 4. Neuron sensitive to both horizontal and vertical disparities. Horizontal disparity was set to the optimal value of 0.75 deg while vertical disparity was varied. This neuron showed a two-dimensional excitatory peak for optimal disparities.

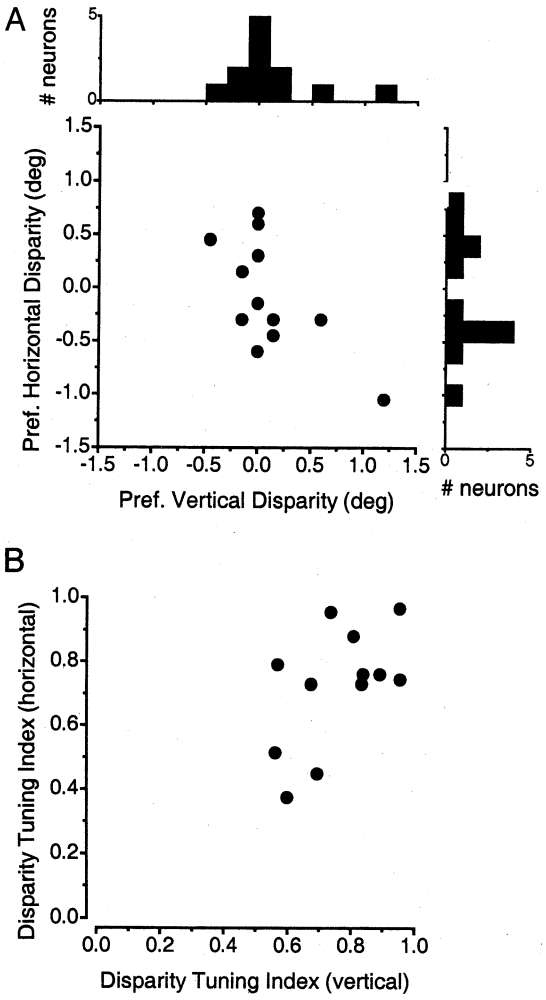

Fig. 5. Comparison of response properties for 12 neurons sensitive to both vertical and horizontal disparity. (A) Preferred vertical and horizontal disparities plotted against each other. (B) Disparity tuning indices plotted against each other.

the vertical-disparity response profile is periodically modulated (i.e. is a Gabor function in terms of the disparity energy model), whereas the horizontal-disparity profile shows no periodicity (i.e. is a Gaussian).

The responses of neuron #1 in Figs. 6A and 6B are consistent with this idea of "true" vertical-disparity detection. Its vertical-disparity tuning curve (Fig. 6A) was periodically modulated (also illustrated by the best Gabor fit). Its horizontal-disparity response profile, however, showed broad (inhibitory) tuning lacking periodic modulation (Fig. 6B). Note also that both tuning curves had comparable baseline activities to nonpreferred disparities (53 and 49 spikes/s for vertical- and horizontal-tuning curves, respectively; derived from the Gabor fit). A similar relationship between vertical- and horizontal-disparity tuning is exhibited by neuron #2 (Figs. 6C and 6D). For neuron #2, the modulation was very broad (large sigma of the Gabor fit), making it difficult to estimate if there was any further modulation for larger horizontal-disparity values. Most cells displayed periodic modulation to both vertical and horizontal disparity. An example is given in Figs. 6E and 6F. The Gabor-like tuning profiles for both vertical and horizontal disparities suggest oblique orientation preference of the monocular subunits of neuron #3.

Discussion

Neurons in the owl's visual Wulst are sensitive to vertical disparities. Tuning profiles to vertical disparities showed periodic modulation and could be fitted well with Gabor functions, very similar to tuning curves derived from horizontal-disparity stimulation. Within the framework of the disparity energy neuron, this suggests that the monocular subunits of these vertical-disparity detectors preferred oblique or even horizontal orientation.

Cells tuned to both vertical and horizontal disparity

According to the widely accepted disparity energy model (Ohzawa et al., 1990, 1997; Qian, 1994; Fleet et al., 1996; Cumming & Parker, 1997; Ohzawa, 1998), the orientation preference of a disparity detector's monocular subunits determines its tuning for vertical, horizontal, and intermediate ("oblique") disparities (see also review by Cumming & DeAngelis, 2001). Only neurons with monocular subunits (simple cells) that show vertical orientation preferences based on the orientation of their Gabor-like RF profile show "true" horizontal-disparity tuning. In other words, a detector's disparity-response profile should exhibit periodic modulation for horizontal disparities, with a disparity modulation frequency analogue to the spatial-frequency filter of its subunits (or input filters, respectively). Such a horizontal-disparity detector, however, would necessarily also be tuned to vertical disparity, as horizontal coincidence of two dots that move far enough will be disrupted. If two dots move vertically further apart than the extension of the disparity detector's RF, a detector will only be stimulated through the subunit in one eye. As a consequence, vertical stimulus displacement will cause a neuron tuned to horizontal disparity to change its firing rate as a function of vertical disparity, but only in a Gauss-like fashion (based on the Gaussian RF envelope) without any periodic modulation. In this case, vertical-disparity tuning is a by-product of the RF extensions. The same considerations hold true for a disparity detector with subunits that prefer horizontal stimulus orientation: Such a neuron will be a "true" vertical-disparity detector showing a periodic modulated (Gabor-like) vertical-disparity tuning profile, but nonperiodic (Gaussian-like) tuning for horizontal disparities. Apart from these extreme cases (pure vertical or horizontal orientation preference), many neurons might show oblique orientation preference. For neurons with oblique orientation preference, the disparity energy model predicts periodically modulated tuning profiles for both vertical and horizontal disparity (in this case, the disparity frequency will be derived from the spatial-frequency selectivity of the subunits, but it will no longer be identical).

To test these predictions of the disparity energy model directly, one should ideally measure responses to a two-dimensional matrix of horizontal- and vertical-disparity values. An alternative approach would be to determine a neuron's tuning to vertical and horizontal disparity in addition to its precise RF size, orientation, and spatial-frequency preferences. Both approaches, however, were too time-consuming to be performed in awake, fixating owls. We, thus, evaluated our data for "true" vertical-disparity tuning by comparing horizontal- and vertical-disparity tuning curves. The fact that the cell shown in Figs. 6A and 6B showed a periodically modulated vertical-disparity tuning curve, but no periodic modulation for horizontal disparities, suggests that "true" vertical-disparity detectors (with horizontal orientation preference of their subunits) exist in the barn owl's brain. The majority of vertical-disparity sensitive cells had Gabor-like profiles to vertical and

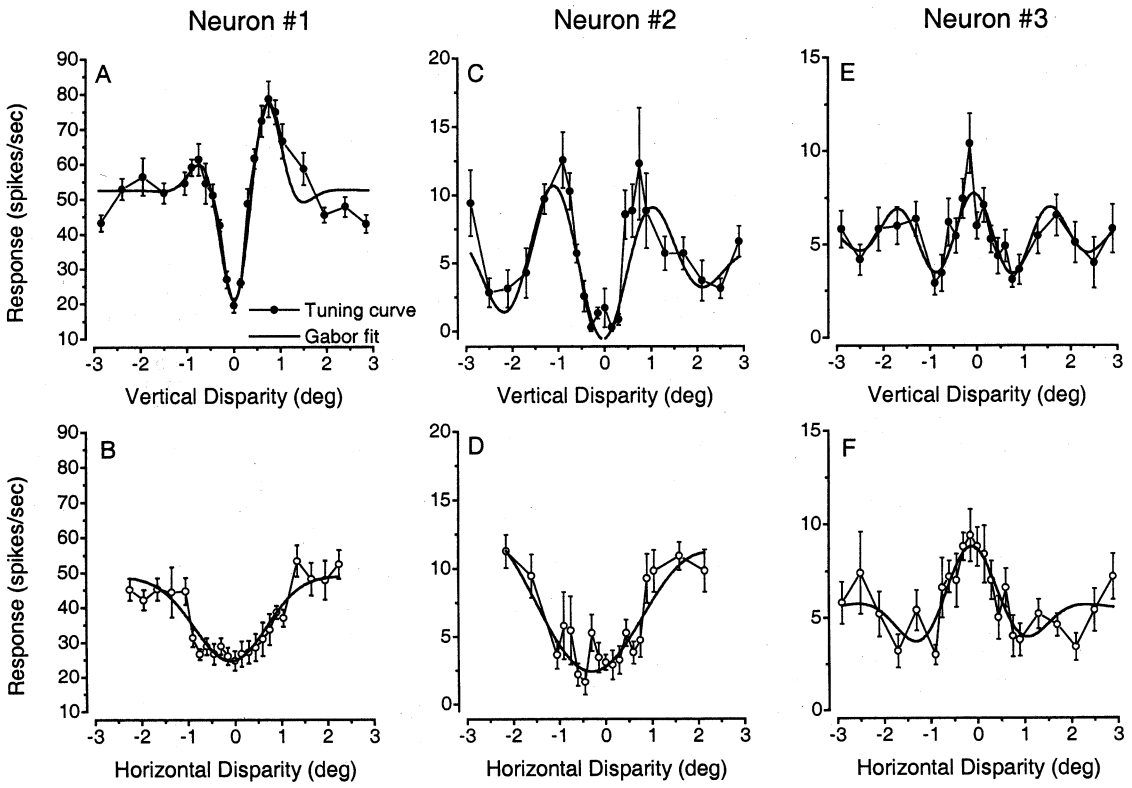

Fig. 6. Tuning of three neurons to both vertical and horizontal disparity. Neuron #1 and #2 showed a periodically modulated vertical-disparity tuning curve (A,C), but no periodic modulation for horizontal disparity (B,D), at least within the measured disparity range. Neuron #3 (same cell as in Fig. 2B) exhibited periodic flank modulation both in the (C) vertical- and (D) horizontal-disparity tuning curve.

horizontal disparity, indicating oblique orientation preference to some extent.

In the feline primary visual cortex, simple cells exhibiting horizontal orientation preference (necessary to generate vertical-disparity detectors) had RF profiles that matched in the left and right eye (DeAngelis et al., 1991, 1995; Ohzawa et al., 1996). This implied that simple cells encode vertical disparity primarily by positional shifts of RFs. For neurons tuned to vertical orientation (required to form horizontal-disparity detectors), on the other hand, the left and right RFs were found to be predominantly dissimilar in shape. This suggested that horizontal disparity is predominantly encoded by means of phase shifts of the RF profiles by cat simple cells. This principle, however, was not confirmed for complex cells in V1 (Anzai et al., 1999).

Comparison to vertical-disparity detectors in mammals

Using bar stimuli, cells sensitive to nonhorizontal disparities have been observed in V1 and V2 of the anesthetized cat (Barlow et al., 1967; Joshua & Bishop, 1970; von der Heydt, 1978), although individual units were not tested for both horizontal- and nonhorizontal-disparity tuning (except for two cells in the study of von der Heydt et al., 1978). Maunsell and Van Essen (1983) for the first time tested various combinations of vertical and horizontal disparities in area MT of the anesthetized monkey. All 19 tested units were sensitive to vertical disparities and their contour plots showed that MT neurons had a single-peaked response profile spanned in the two-dimensional disparity domain. Using RDS in the fixating monkey, Gonzalez and colleagues (1993) found that 30% of V1 cells and 41% of V2 cells were responsive to both horizontal and vertical disparities. Cells responded either to both disparities or to none of them. Interestingly, most cells (70%) in the study by Gonzalez et al. (1993) were vertical *tuned inhibitory* types—thus suppressed at zero degree of vertical disparity—whereas most neurons in the current study showed profiles with an excitatory peak near zero degree of vertical disparity. Finally, neurons in area V3–V3A of the fixating monkey are also sensitive to vertical disparity (Poggio, 1995). Because of a quite restricted range of tested disparity values (in the range of ± 1 deg), the presence or absence of periodic modulation in vertical-disparity profiles in primate studies is hard to estimate and, thus, artefactual tuning caused by disruption of horizontal-disparity tuning is difficult to exclude.

Possible role of vertical-disparity coding in the owl

Early in development, the eyes of barn owls are exodeviant and thus, visual feedback (i.e. fused binocular vision) during development is essential for appropriate alignment of the eyes (Knudsen, 1989). In owls that were strabismic due to early monocular lid suture, binocularly driven Wulst neurons (and as a consequence, disparity-sensitive neurons) were absent (Pettigrew & Konishi, 1976*b*). As the horopter (with its horizontal and vertical dimensions) is the locus point around which stereoscopic depth perception is possible, developmental processes should include not only suitable interocular positioning, but also precise vertical eye

alignment. Cells tuned to vertical disparity may provide an instructional signal about the vertical positioning of the eyes. Apart from this hypothetical role of vertical-disparity coding during development, the function of vertical-disparity coding in adult owl is unknown. Future behavioral studies may help to elucidate if vertical disparity is used to estimate the absolute distance of objects, as has been suggested in humans.

Acknowledgments

We thank Rob van der Willigen and Bernhard Gaese for supporting software development. Kathleen C. Anderson and Joerg Lippert read an earlier version of the paper. Two anonymous referees provided helpful comments on the manuscript. This research was supported by a grant from the DFG to H. Wagner (WA606/6).

References

ANZAI, A., OHZAWA, I. & FREEMAN, R.D. (1999). Neural mechanisms for processing binocular information. II. Complex cells. *Journal of Neurophysiology* **82**, 909–924.

BARLOW, H.B., BLAKEMORE, C. & PETTIGREW, J.D. (1967). The neural mechanisms of binocular depth discrimination. *Journal of Physiology* (London), **193**, 327–342.

BRADSHAW, M.F., GLENNERSTER, A. & ROGERS, B.J. (1996). The effect of display size on disparity scaling from differential perspective and vergence cues. *Vision Research* **36**, 1255–1264.

COOPER, M.L. & PETTIGREW, J.D. (1979). A neurophysiological determination of the vertical horopter in the cat and owl. *Journal of Comparative Neurology* **184**, 1–26.

CUMMING, B.G. & DEANGELIS, G.C. (2001). The physiology of stereopsis. *Annual Review of Neuroscience* **24**, 203–238.

CUMMING, B.G. & PARKER, A.J. (1997). Responses of primary visual cortical neurons to binocular disparity without depth perception. *Nature* **389**, 237–280.

CUMMING, B.G., JOHNSTON, E.B. & PARKER, A.J. (1991). Vertical disparities and perception of three-dimensional shape. *Nature* **349**, 411–413.

DEANGELIS, G.C., OHZAWA, I. & FREEMAN, R.D. (1991). Depth is encoded in the visual cortex by a specialized receptive field structure. *Nature* **352**, 156–159.

DEANGELIS, G.C., OHZAWA, I. & FREEMAN, R.D. (1995). Neuronal mechanisms underlying stereopsis: How do simple cells in the visual cortex encode binocular disparity? *Perception* **24**, 3–31.

DU LAC, S. & KNUDSEN, E.I. (1990). Neural maps of head movement vector and speed in the optic tectum of the barn owl. *Journal of Neurophysiology* **63**, 131–146.

FELDMAN, D.E., BRAINARD, M.S. & KNUDSEN, E.I. (1996). Newly learned auditory responses mediated by NMDA receptors in the owl inferior colliculus. *Science* **271**, 525–528.

FLEET, D.J., WAGNER, H. & HEEGER, D.J. (1996). Neural encoding of binocular disparity: Energy models, position shifts and phase shifts. *Vision Research* **36**, 1839–1857.

GABOR, D. (1946). Theory of communication. *Journal of the Institute of Electrical Engineers* **93**, 429–457.

GONZALEZ, F., RELOVA, J.L., PEREZ, R., ACUNA, C. & ALONSO, J.M. (1993). Cell responses to vertical and horizontal retinal disparities in the monkey visual cortex. *Neuroscience Letters* **160**, 167–170.

HOWARD, I.P. & ROGERS, B.J. (1995). *Binocular Vision and Stereopsis*. Oxford: Oxford University Press.

JOSHUA, D.E. & BISHOP, P.O. (1970). Binocular single vision and depth discrimination. Receptive field disparities for central and peripheral vision and binocular interaction on peripheral units in cat striate cortex. *Experimental Brain Research* **10**, 389–416.

JULESZ, B. (1960). Binocular depth perception of computer-generated patterns. *Bell Systems Technical Journal* **39**, 1125–1162.

KARTEN, H.J., HODOS, W., NAUTA W.J.H. & REVZIN, A.M. (1973). Neural connections of the "visual Wulst" of the avian telencephalon. Experimental studies in the pigeon (*Columba livia*) and owl (*Speotyto cunicularia*). *Journal of Comparative Neurology* **150**, 253–278.

KNUDSEN, E.I. (1989). Fused binocular vision is required for development of proper eye alignment in barn owls. *Visual Neuroscience* **2**, 35–40.

LAMME, V.A.F., ZIPSER, K. & SPEKREIJSE, H. (1998). Figure-ground activity in primary visual cortex is suppressed by anesthesia. *Proceedings of the National Academy of Sciences of the U.S.A.* **95**, 3263–3268.

MAUNSELL, J.H.R. & VAN ESSEN, D.C. (1983). Functional properties of neurons in the middle temporal visual area of the macaque monkey. II. Binocular interactions and sensitivity to binocular disparity. *Journal of Neurophysiology* **49**, 1148–1167.

MAYHEW, J. & LONGUET-HIGGINS, H.C. (1982). A computational model of binocular depth perception. *Nature* **297**, 376–378.

NAKAYAMA, K. (1977). Geometrical and physiological aspects of depth perception. In *Three-Dimensional Imaging*, ed. BENTON, S.A., pp. 1–8. Society of Photo-Optical Instrumentation Engineers Proceedings 120, Bellingham, Washington.

NIEDER, A. & WAGNER, H. (2000). Horizontal-disparity tuning of neurons in the visual forebrain of the behaving barn owl. *Journal of Neurophysiology* **83**, 2967–2979.

NIEDER, A. (2000). Miniature stereo radio transmitter for simultaneous recording of multiple single-neuron signals from behaving owls. *Journal of Neuroscience Methods* **101**, 157–164.

OHZAWA, I. (1998). Mechanisms of stereoscopic vision: The disparity energy model. *Current Opinion in Neurobiology* **8**, 509–515.

OHZAWA, I., DEANGELIS, G.C. & FREEMAN, R.D. (1990). Stereoscopic depth discrimination in the visual cortex: Neurons ideally suited as disparity detectors. *Science* **249**, 1037–1040.

OHZAWA, I., DEANGELIS, G.C. & FREEMAN, R.D. (1996). Encoding of binocular disparity by simple cells in the cat's visual cortex. *Journal of Neurophysiology* **75**, 1779–1805.

OHZAWA, I., DEANGELIS, G.C. & FREEMAN, R.D. (1997). Encoding of binocular disparity by complex cells in the cat's visual cortex. *Journal of Neurophysiology* **77**, 2879–2909.

ORBAN, G.A. (1991). Quantitative electrophysiology of visual cortical neurones. In *Vision and Visual Dysfunction, Vol. 4: The Neural Basis of Visual Function*, ed. CRONLY-DILLON, J., pp. 173–222. New York: MacMillan.

PETTIGREW, J.D. & KONISHI, M. (1976*a*). Neurons selective for orientation and binocular disparity in the visual Wulst of the barn owl (*Tyto alba*). *Science* **193**, 675–678.

PETTIGREW, J.D. & KONISHI, M. (1976*b*). Effects of monocular deprivation on binocular neurons in the owl's visual Wulst. *Nature* **264**, 753–754.

PETTIGREW, J.D. (1979). Binocular visual processing in the owl's telencephalon. *Proceedings of the Royal Society* (London) **204**, 435–454.

PETTIGREW, J.D. (1986). The evolution of binocular vision. In *Visual Neuroscience*, ed. PETTIGREW, J.D., SANDERSON, K.J. & LEVICK, W.R., pp. 208–222. Cambridge: Cambridge University Press.

POGGIO, G.F. (1995). Mechanisms of stereopsis in monkey visual cortex. *Cerebral Cortex* **3**, 193–204.

QIAN, N. (1994). Computing stereo disparity and motion with known binocular cell properties. *Neural Computation* **6**, 390–404.

ROGERS, B.J. & BRADSHAW, M.F. (1993). Vertical disparities, differential perspective and binocular stereopsis. *Nature* **361**, 253–255.

STEINBACH, M.J. & MONEY, K.E. (1973). Eye movements of the owl. *Vision Research* **13**, 889–891.

VAN DER WILLIGEN, R.F., FROST, B.J. & WAGNER, H. (1998). Stereoscopic depth perception in the owl. *Neuroreport* **9**, 1233–1237.

VON DER HEYDT, R., ADORJANI, C.S., HAENNY, P. & BAUMGARTNER, G. (1978). Disparity sensitivity and receptive field incongruity of units in cat striate cortex. *Experimental Brain Research* **31**, 523–545.

WAGNER, H. & SCHAEFFEL, F. (1991). Barn owls use accommodation as a distance cue. *Journal of Comparative Physiology A* **169**, 515–521.